

Article

Nitrate Removal from Groundwater by Heterotrophic and Electro-Autotrophic Denitrification

Shuangshuang Yao, Lei Liu, Shiyang Zhang  and Xinhua Tang *

School of Civil Engineering and Architecture, Wuhan University of Technology, No.122 Luoshi Road, Hongshan District, Wuhan 430070, China; yaoshuangshuang@whut.edu.cn (S.Y.); 13125177038@163.com (L.L.); zhangshiyang7@126.com (S.Z.)

* Correspondence: tangxinhua@whut.edu.cn

Abstract: A heterotrophic and autotrophic denitrification (HAD) system shows satisfactory performance for groundwater with nitrate contamination. In this study, an HAD system combining solid-phase heterotrophic denitrification and electrochemical hydrogen autotrophic denitrification (SHD-EHD) was developed for the treatment of nitrate-contaminated groundwater, in which polycaprolactone (PCL) was used as the carbon source to enhance the nitrate removal performance and prevent secondary pollution of the electrochemical hydrogen autotrophic denitrification (EHD) system. The denitrification performance, microbial community structure and nitrogen metabolism were investigated. The results showed that a high nitrate removal rate of 99.04% was achieved with an influent nitrate concentration of 40 mg/L, a current of 40 mA and a hydraulic retention time (HRT) of 4 h. By comparing the performance with the EHD system, it was found that the HAD system with PCL promoted the complete denitrification and reduced the accumulation of NO_2^- -N. Analysis of the microbial community structure identified the key denitrifying bacteria: *Dechloromonas*, *Thauera* and *Hydrogenophaga*. A comparison of microbial communities from SHD-EHD and solid-phase heterotrophic denitrification (SHD) demonstrated that electrical stimulation promoted the abundance of the dominant denitrifying bacteria and the electroactive bacteria. Analysis of the nitrogen metabolic pathway revealed that the conversion of NO to N_2O was the rate-limiting step in the overall denitrification pathway. The SHD-EHD developed in this study showed great potential for groundwater nitrate removal.

Keywords: nitrate; biofilm electrode reactor; hydrogen autotrophic denitrification; solid-phase heterotrophic denitrification; microbial community



Citation: Yao, S.; Liu, L.; Zhang, S.; Tang, X. Nitrate Removal from Groundwater by Heterotrophic and Electro-Autotrophic Denitrification. *Water* **2022**, *14*, 1759. <https://doi.org/10.3390/w14111759>

Academic Editors: Minhua Cui and Guoshuai Liu

Received: 29 April 2022

Accepted: 27 May 2022

Published: 30 May 2022

Publisher's Note: MDPI stays neutral with regard to jurisdictional claims in published maps and institutional affiliations.



Copyright: © 2022 by the authors. Licensee MDPI, Basel, Switzerland. This article is an open access article distributed under the terms and conditions of the Creative Commons Attribution (CC BY) license (<https://creativecommons.org/licenses/by/4.0/>).

1. Introduction

Groundwater represents 99% of the world's liquid freshwater and is the source of one quarter of all the water used by humans [1]. Two billion people still lack access to safe drinking water, and groundwater plays a significant role in sustainable development according to the Sustainable Development Goals (SDGs) from the United Nations [2]. Human production activities are the main reason for the contamination of nitrate in groundwater. Excessive application of chemical fertilizers, uncontrolled discharge of industrial/domestic wastewater and infiltration of waste leachate all contribute to nitrate pollution in groundwater [3]. These contaminations not only affect water systems worldwide [4], but also threaten human health. Nitrate can be transformed to nitrite in the human body, which may lead to methemoglobinemia; nitrite can be further converted to nitrosamine, increasing the risk of cancer [5]. There have been many reports of nitrate contamination around the world, such as in eastern Nebraska in USA and in the Yellow River Delta in China [6]. The maximum concentration of nitrate and nitrite regulated by China are 10 mg/L NO_3^- -N and 1 mg/L NO_2^- -N, respectively (GB5749-2022).

Nitrogen in water undergoes migration and transformation under biological and chemical processes. Denitrification is a significant process of the nitrogen cycle, as well

as in the biological treatment of nitrate in groundwater [7]. Among various methods for nitrate removal, biofilm electrode reactor (BER) has attracted increasing attention due to its satisfactory performance [8,9]. However, heterotrophic denitrification has the problem of secondary pollution caused by added organic carbon source [10]. In situ electrochemical hydrogen production realized by BER overcomes the disadvantages of low H₂ mass transfer rate of conventional autotrophic denitrification and eliminates the risks of H₂ during transportation and operation. However, the processing capacity of BER is affected by the reactor configuration [11] and the supply of inorganic carbon sources [12]. The BER also consumes a lot of electrical energy to produce CO₂ and H₂. In addition, the acclimatization of autotrophic microorganisms is time-consuming and the biofilm is easy to shed. The difference in current intensity (I) and hydraulic retention time (HRT) affects the number, species, activity and metabolism of microorganisms on the biofilm, thus influencing nitrate removal rate and accumulation of nitrite [13].

To further improve the processing capacity of BER, researchers increased the cathode surface area and adapted reactor operating conditions, such as dicyclic-type electrode based biofilm reactor [14], upflow BER [15], and added microbial carriers such as fiber threads [12,16] and wheat-rice stone powder [17]. In addition, researchers developed an enhanced biofilm electrode reactor that combined autotrophic and heterotrophic denitrification, which provided adequate inorganic carbon for autotrophic denitrification [18,19]. Moreover, it has been demonstrated that heterotrophic and autotrophic denitrification (HAD) can be realized synergistically [16]. In an HAD system, heterotrophic denitrification combined with autotrophic denitrification reduces the consumption of organic carbon to some extent [18], overcoming the weaknesses of secondary pollution and blockage in the reactor. External carbon sources currently used for HAD are mainly liquid-phase carbon sources such as glucose, ethanol, methanol and acetate [20]. Although liquid-phase carbon sources are effective for heterotrophic denitrification, the dosing of carbon source is easily influenced by fluctuations of influent quality, and the system requires complicated online monitoring and control instruments [21]. To solve the above problems, the recently developed solid-phase carbon source denitrification technology, which uses biodegradable polymers as carbon sources and biofilm carriers as well, has shown a promising potential in the removal of nitrate from groundwater. These biodegradable polymers are polymeric compounds formed by covalent bonding of monomer substances that can easily be hydrolyzed by enzymes of bacteria or fungi [22,23]. Many biodegradable polymers, such as polyhydroxyalkanoates (PHAs) [24,25], polycaprolactone (PCL) [26,27] and polybutylene succinate (PBS) [28,29], have been used for solid-phase denitrification and have exhibited satisfactory performance. However, few studies on the combination of heterotrophic denitrification using biodegradable polymers and electrochemical hydrogen autotrophic denitrification have been reported.

Considering the above-mentioned aspects, an HAD system with a solid-phase heterotrophic denitrification and electrochemical hydrogen autotrophic denitrification (SHD-EHD) was constructed for the treatment of nitrate-contaminated groundwater. PCL was used as the solid carbon source for denitrification. PCL is insoluble in water and has good hydrophobicity, but it can be hydrolyzed by microbial enzymes. The amount of hydrolyzed PCL is determined by the number of microorganisms in the reactor, so there is no need to artificially control the dosing of PCL. In addition, the hydrolyzed products of PCL are CO₂ and H₂O, which can continuously provide a carbon source for autotrophic denitrification.

A comparison between the start-up of the SHD-EHD and the BER was studied. The effects of current intensity (I) and HRT on nitrate removal from groundwater by SHD-EHD were investigated to optimize the system. Under the optimal conditions, the water quality indices and microbial communities were studied to evaluate the transformation and synergistic degradation mechanism of nitrate in SHD-EHD. This study aimed to provide an effective method to remove nitrate from groundwater, which was in line with the target of “improving water quality by reducing pollution” in the SDGs.

2. Materials and Methods

2.1. Materials

The physical characteristics of PCL granules (Capa 6800, Solvay Corporation, Pasadena, CA, USA) were as follows: shape (ellipsoidal), diameter (2–3 mm), average weight (0.0123 g per piece), mass density (1.15 g/cm³), molecular weight (80,000 Da).

The simulated nitrate-contaminated groundwater (1 L deionized water) contained 0.243 g NaNO₃ (40 mg/L NO₃⁻-N). Appropriate amounts of mineral elements (23 mg/L MgSO₄·7H₂O, 131 mg/L NaHCO₃, 13 mg/L Na₂HPO₄, 158 mg/L MgCl₂·6H₂O) were added to the simulated groundwater for microbial growth.

2.2. Experimental Apparatus

The experimental apparatus consisted of a laboratory-scale SHD-EHD, a DC regulated power supply, a peristaltic pump and two storage tanks (Figure 1). The SHD-EHD was made by a PVC cylinder (9 cm in diameter and 29 cm in height) with an effective volume of 2 L, in which two baffles were set at the bottom and the top of the reactor to fix the electrodes and achieve uniform water distribution. A graphite rod (1 cm in diameter and 30 cm in length) was placed in the center of the cylindrical reactor to serve as the anode, while a 3 mm thick carbon felt was in a circle against the inner wall of the reactor as the cathode. Carbon felt has been widely used as electrode material due to its good biocompatibility, satisfactory conductivity and low cost [30]. The utilization of the carbon rod anode was ascribed to its good conductivity and biochemical stability. The flow rate of influent and effluent were controlled by a multi-channel peristaltic pump (BT600S, Leadfluid, Baoding, China). A DC power supply (IT6302, Itech, Nanjing, China) was applied to provide constant DC power for different operating conditions. The lower section of the reactor was filled with plastic multifaceted hollow spheres to support PCL. As the control, SHD was the same as SHD-EHD without current application.

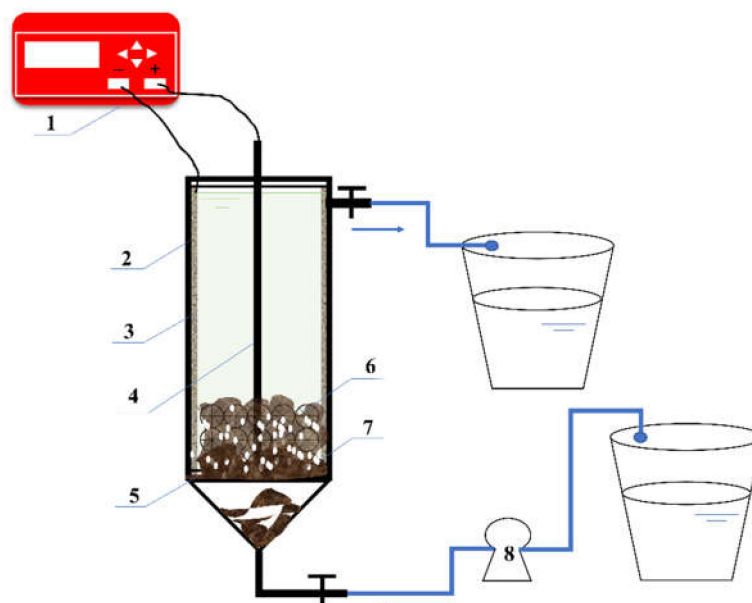


Figure 1. Experimental apparatus. 1 DC Power supply; 2 Reactor; 3 Cathode: Carbon felt; 4 Anode: Graphite rod; 5 Supporting board; 6 PCL; 7 Biofilm; 8 Peristaltic pump.

2.3. Experimental Start-Up and Operation

The experiments were divided into the following parts: EHD start-up and operation (stage I); SHD-EHD start-up and operation (stage II). Detailed operations are presented below. All experiments were conducted under room temperature.

EHD start-up: First, 0.5 L of activated sludge from Beihu wastewater treatment plant (Wuhan, China) was inoculated into the EHD. In the early stage of start-up, the EHD

was operated under the sequence batch mode without applying current. The synthetic groundwater containing 30 mg/L NO_3^- -N was replaced every 12 h and the pH was adjusted to neutral. After 15 days of anaerobic cultivation, the current was applied to acclimatize the microorganisms in the reactor. The current intensity gradually increased from 1 mA to 100 mA, and the feed mode was changed to continuous flow with an HRT of 12 h. The start-up was basically considered complete when nitrate removal rate reached 75%.

Stage I: The denitrification performances under different current intensities, HRT, influent pH and influent NO_3^- -N concentrations were tested to obtain optimal operating conditions of the EHD, which also provided guidance for the SHD-EHD operating. The experimental conditions and performance of the EHD were summarized in Figure S1.

SHD-EHD start-up: The collected activated sludge was first inoculated into the SHD-EHD. Different from the EHD, the NO_3^- -N concentration of the synthetic groundwater was 40 mg/L and replaced every 10 h during the start-up. Other procedures were the same as EHD start-up except that the applied current intensity increased from 10 mA to 40 mA.

Stage II: The influences of current intensity and HRT on the denitrification performance of the SHD-EHD were studied. The influent pH was controlled at about 7.5. Detailed influent conditions were shown in Table 1.

Table 1. Operation parameters of SHD-EHD.

Days	I (mA)	HRT (h)	inf- NO_3^- -N (mg/L)	Days	I (mA)	HRT (h)	inf- NO_3^- -N (mg/L)
1~8	5	10	40	1~7	40	2.5	40
9~16	10	10	40	8~14	40	3.0	40
17~25	20	10	40	15~22	40	3.5	40
26~34	30	10	40	23~30	40	4.0	40
35~43	40	10	40	31~38	40	4.5	40

The nitrate removal rate (η , %) and the denitrification rate (R , mg NO_3^- -N/(cm²·d)) were calculated as follows:

$$\eta = \frac{C_0 - C_t}{C_0} \times 100\% \quad (1)$$

$$R = \frac{Q \times (C_0 - C_t) \times 24}{A} \quad (2)$$

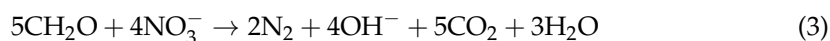
where C_0 is the initial NO_3^- -N concentration (mg/L); C_t is the NO_3^- -N concentration at time t (mg/L); Q is the influent flow rate (L/h); A is the cathode surface area (cm²).

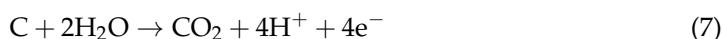
2.4. Analytical Methods

Influent and effluent samples were collected and analyzed according to standard methods. All samples were filtered using 0.45 μm filter before analyses. Concentrations of NO_3^- -N, NO_2^- -N and TN were analyzed using a UV spectrophotometer (HACH, DR 5000, Loveland, CO, USA). pH was measured by a pH meter (SIN-CT6321, Sinomeasure, Hangzhou, China). High-throughput Sequencing was conducted at Majorbio Technology CO., LTD. (Shanghai, China) and the detailed procedures were presented in Supplementary Materials.

2.5. Chemical Equations

Chemical equations related to material conversion and mechanism were as follows:





3. Results and Discussion

3.1. Start-Up of the EHD and SHD-EHD

As showed in Figure 2, the nitrate removal rate was positively correlated with the current intensity during the start-up period of the EHD. When the current intensity was adjusted to 70 mA and maintained for 7 days at an HRT of 12 h, the nitrate removal rate could be higher than 75%, and tawny biofilm was observed on the cathode, which was regarded as the completion of the start-up. The whole process took about 60 days.

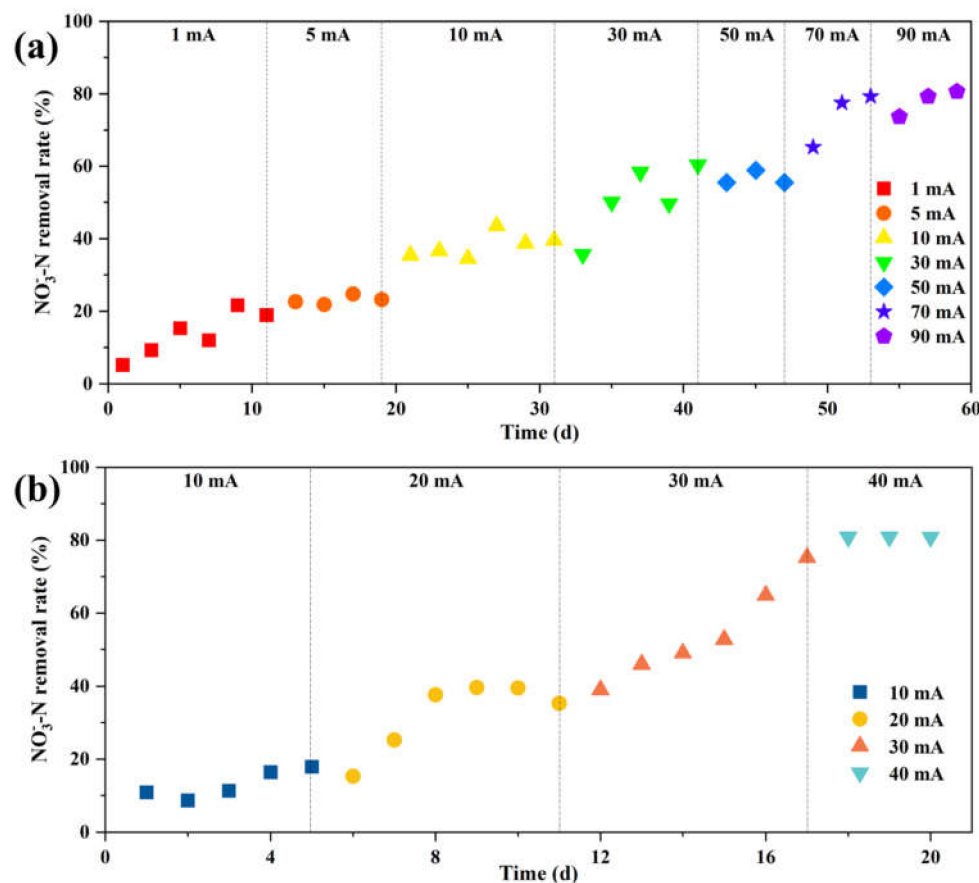


Figure 2. Nitrate removal rate during the start-up of (a) EHD; (b) SHD–EHD.

For the start-up of the SHD-EHD, when the current intensity was adjusted to 30 mA and maintained for 7 days at an HRT of 10 h, the nitrate removal rate could be more than 75% and tawny biofilm was observed on both PCL and the cathode (Figure S2), which was regarded as the completion of the start-up. The whole process took about 22 days. The time required for the start-up of the SHD-EHD was considerably shorter compared with the EHD, while the required current was smaller. These results indicate that the SHD-EHD not only achieved fast start-up to overcome the disadvantage of the long start-up of the EHD, but also realized high removal rate in treating simulated groundwater.

3.2. Optimization of the EHD Operating Parameters

In stage I, the operating parameters such as the current intensity, HRT, influent pH and influent NO₃⁻-N concentration of EHD were optimized. The influent NO₃⁻-N concentration was set to 30 mg N/L. The operating parameters and overall performance of the EHD were presented in Figure S1.

The nitrate removal rate increased with the increase of current intensity in the range of 10–86 mA. When the current intensity was set to 86 mA, the nitrate removal rate reached

a maximum of 90.80%. A decreasing trend was observed after the current intensity was greater than 86 mA. This might be due to the occurrence of “hydrogen inhibition” caused by high concentration of H_2 generated under high current intensity, which reduced the microbial activity [31]. The NO_2^- -N accumulation kept growing as the current intensity increased from 10 mA to 90 mA (Figure S3).

When $HRT < 9$ h, the nitrate removal rate was positively correlated with HRT, rising from 43.33% to 90.12%. When $HRT > 9$ h, the influence of HRT on the nitrate removal rate was gradually weakened. The nitrate removal rate and the effluent NO_2^- -N concentration remained stable (Figure S4).

The pH range suitable for the EHD was weakly alkaline (pH 7.45–8.1) (Figure S5). The EHD had a buffering capacity for pH variations due to CO_2 production by electrolysis of the carbon rod anode (Figure S6).

When the influent NO_3^- -N concentration was lower than 40 mg/L, the removal amount of NO_3^- -N increased markedly with the increase of influent NO_3^- -N concentration. When the NO_3^- -N concentration was 40~60 mg/L, the removal amount of NO_3^- -N still increased but the increase rate was much smaller. The removal amount of NO_3^- -N decreased when the concentration of influent NO_3^- -N was higher than 60 mg/L (Figure S7).

To sum up, the optimal operating parameters for the EHD in this study were as follows: current intensity of 86 mA~96 mA; HRT of 9 h; influent pH of 7.45~8.1; influent NO_3^- -N concentration of 40 mg N/L. Under these conditions, the nitrate removal rate ranged from 80% to 90%, while both the effluent NO_3^- -N concentration and the effluent NO_2^- -N concentration was 4~6 mg/L. This provided a reference for the following study of the range of the current and HRT for SHD-EHD.

3.3. Effect of Current Intensity on Performance of the SHD-EHD

As shown in Figure 3, the NO_3^- -N and TN concentrations in the effluent gradually declined with the growth of current intensity under an HRT of 9 h. When the current intensity increased from 5 mA to 40 mA, the nitrate removal rate increased from 50.30% to 86.53% and the TN removal rate increased from 15.30% to 78.72%. The main reason for the growth of the nitrogen removal rate was that the boost of current intensity promoted the generation of H_2 on the cathode and CO_2 on the anode, which served as the electron donor and inorganic carbon source for the autotrophic microorganisms, respectively. In addition, the increase of current intensity could facilitate the activity of denitrification microorganisms [16] and stimulate the activity of nitrate reductase in autotrophic microorganisms [32], thus enhancing the utilization of H_2 by autotrophic microorganisms and improving the denitrification rate of the SHD-EHD. When the current intensity increased from 30 mA to 40 mA, the increase in the nitrate removal rate was not obvious. Further increase of current intensity might cause a waste of electrical energy. Moreover, the applied current intensity should not be too high to inhibit the bacterial activity; it was confirmed that high current density (>320 mA/m²) would inhibit the activity of microorganisms in a SHD-EHD system [16]. With the rising current, the concentration of NO_2^- -N in the effluent gradually increased from 0.2 mg/L to 0.62 mg/L. The possible reasons were as follows: short HRT and insufficient electron donor lead to incomplete denitrification; nitrite reductase was less capable of competing for electrons than nitrate reductase. Therefore, in an unstable environment, denitrifying bacteria tended to use NO_3^- -N as the terminal electron acceptor instead of NO_2^- -N, leading to the accumulation of NO_2^- -N.

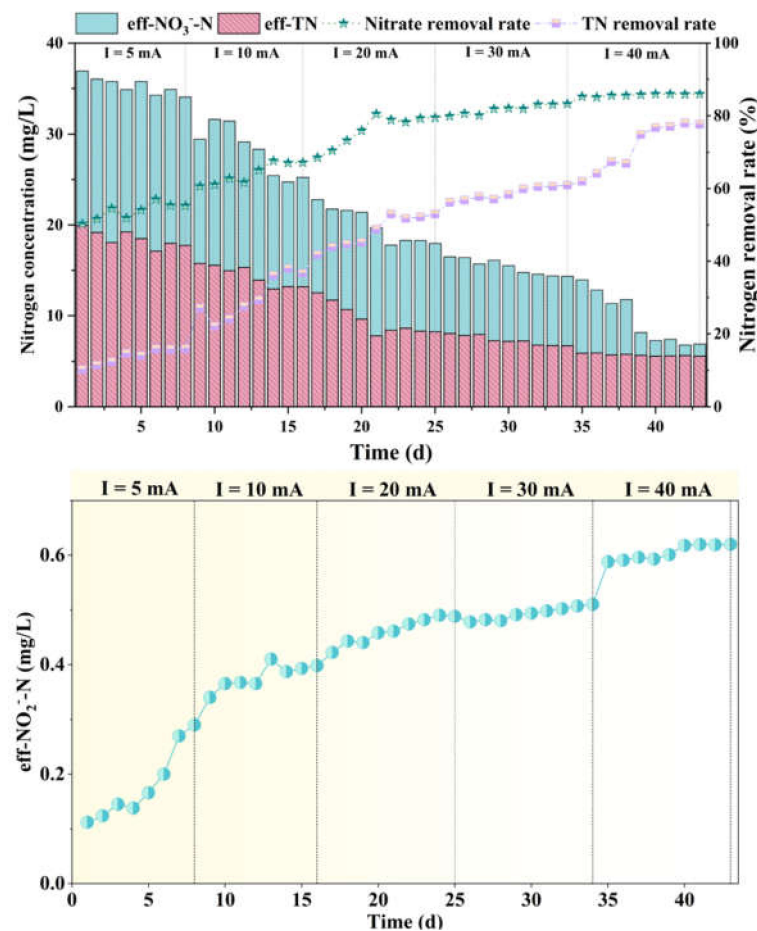


Figure 3. Concentrations of NO_3^- -N, TN and NO_2^- -N, nitrate removal rate in the SHD-EHD at different current intensities.

3.4. Effect of HRT on Performance of the SHD-EHD

As shown in Figure 4, the effluent concentrations of NO_3^- -N, NO_2^- -N and TN all declined with the increase of HRT. When the HRT increased to 4 h, the effluent NO_2^- -N concentration was low and the nitrate removal rate reached 90%. With the extension of HRT, the nitrogen removal rate of the SHD-EHD improved obviously.

HRT is one of the key parameters of an SHD-EHD system, which determines the treatment capacity of the reactor at a certain influent flow rate. The longer the HRT, the more the bacteria can remove NO_3^- -N. In the study of the EHD, 92.36% of NO_3^- -N could be removed at an HRT of 9 h when the influent NO_3^- -N concentration was 30 mg/L. The nitrate removal rate of the SHD-EHD achieved 94.02% at an HRT of 4 h when the influent NO_3^- -N concentration was 40 mg/L. Obviously, the SHD-EHD could enhance the nitrate removal rate.

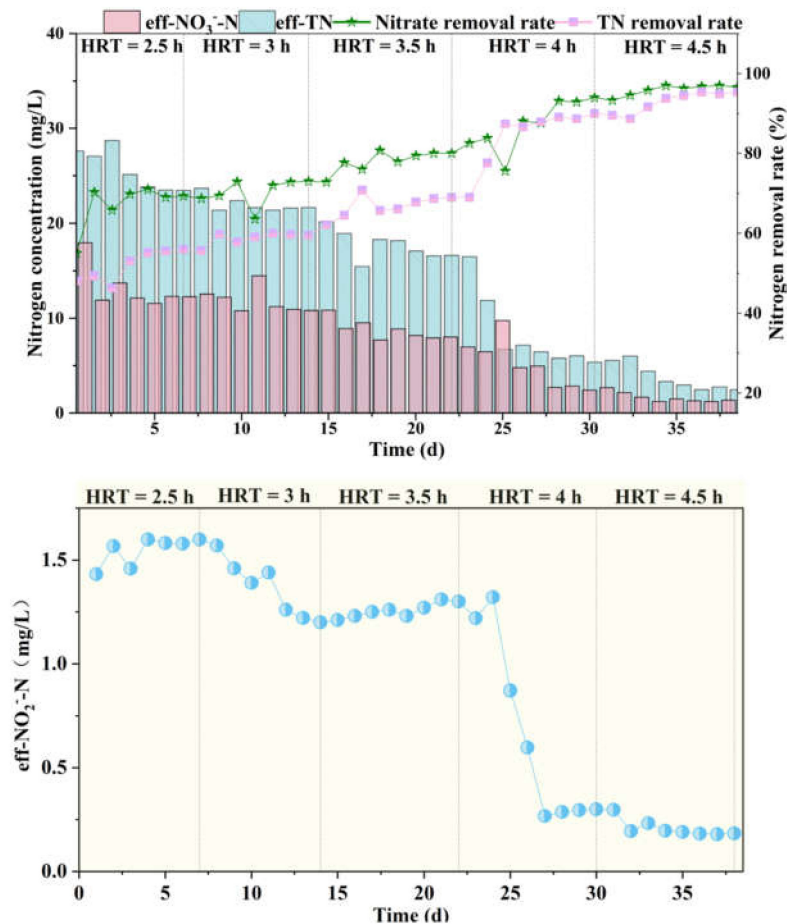


Figure 4. Concentrations of NO_3^- -N, TN and NO_2^- -N, nitrate removal rate in the SHD-EHD at different HRT.

3.5. pH Variation

Figure 5 shows the pH variation of the SHD-EHD under different current intensity and HRT. It could be seen that the effluent pH remained between 7 and 8.25. The effluent pH reduced from 8.22 to 7.05 when the current intensity increased from 5 mA to 40 mA. The effluent pH increased from 7.44 to 8.25 when the HRT boosted from 2.5 h to 4.5 h.

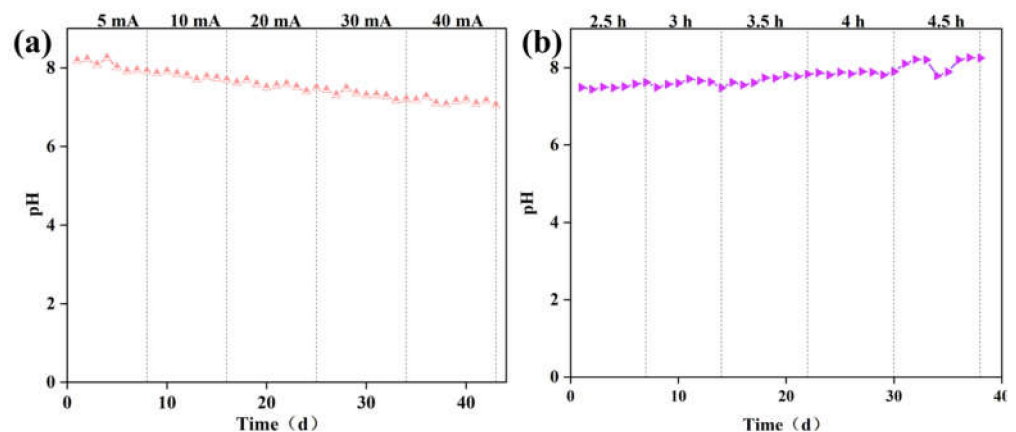


Figure 5. Variation of pH under different (a) Current intensities; (b) HRT.

According to the calculation, the removal of 1 mol NO_3^- -N produced 3.57 mg of alkalinity (CaCO_3). Therefore, the pH in the reactor would increase as the treatment

proceeded. However, the effluent pH showed small fluctuations and finally stabilized between 7 and 8.25, indicating that the SHD-EHD had good pH buffering capacity. Possible reasons were as follows:

- H^+ and CO_2 were generated by the electrochemical reaction between the carbon rod anode and H_2O . The generated H^+ neutralized the alkalinity produced by denitrification, while the CO_2 combined with OH^- in water and existed in the form of HCO_3^- , which endowed the reactor with good pH buffering capacity;
- Solid-phase heterotrophic denitrification could also produce CO_2 , which reacted with OH^- to reduce the alkalinity. This also provided a stable pH favorable for denitrification.

3.6. Denitrification Performance of the SHD-EHD under Optimal Conditions

From the above nitrate removal and NO_2^- -N accumulation study, it could be concluded that the optimal condition of the SHD-EHD was as follows: current intensity of 40 mA, HRT of 4 h, influent pH of 7.4~7.5 and influent NO_3^- -N concentration of 40 mg/L. The SHD-EHD was operated under this condition for 43 days, and the results are shown in Figure 6. Under the optimal condition, the nitrate removal rate of the SHD-EHD was above 90% and the highest nitrate removal rate reached 99.04%. The effluent NO_3^- -N concentration ranged from 1.41 mg/L to 3.76 mg/L and the effluent NO_2^- -N concentration ranged from 0.27 mg/L to 0.62 mg/L. Compared with the EHD, the SHD-EHD was able to obtain a higher nitrate removal rate in a shorter HRT. The SHD-EHD reactor also increased the denitrification rate and reduced the NO_2^- -N concentration in the effluent (Figure 7). It indicated that the addition of PCL facilitated the removal of NO_3^- -N and enhanced the complete denitrification in groundwater. These results demonstrate that the SHD-EHD could effectively remove NO_3^- -N.

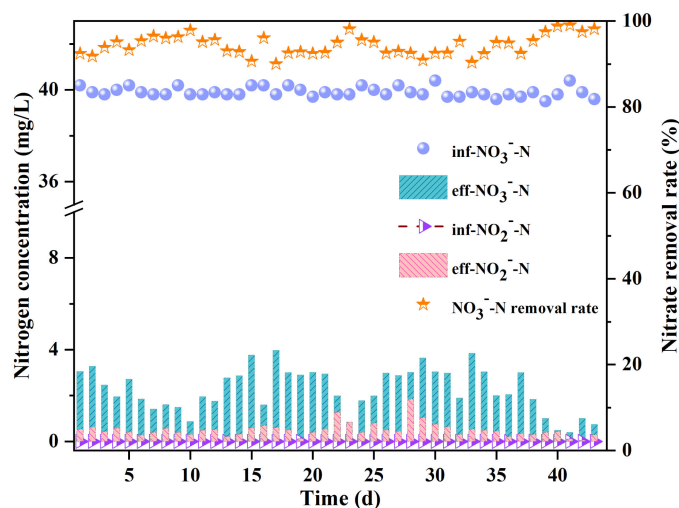


Figure 6. Denitrification performance of SHD–EHD under optimal conditions ($I = 40$ mA, HRT = 4 h, pH = 7.4~7.5, inf- NO_3^- -N = 40 mg/L).

A comparison of nitrate removal rate in different HAD systems was presented in Table 2. The SHD-EHD in this study achieved a satisfactory nitrate removal rate within a much shorter HRT when the influent NO_3^- -N concentrations were similar. Tong et al. [33] filled the reactor with pine sawdust and haycite as solid carbon sources and biocarriers; the HRT required to achieve satisfactory nitrate removal rate was longer than the SHD-EHD in this study. This might be due to the fact that some natural biopolymer materials were difficult to be utilized by microorganisms. A previous study suggested that denitrification rates using lignocellulosic materials as electron donors were usually lower than those of conventional liquid-phase organics (such as glucose and ethanol) [34] while PCL could reach a similar performance to liquid-phase organics. In most reported studies, biodegrad-

able polymers as carbon sources achieved higher denitrification performance than that of natural biopolymer materials [26]. Compared with the results of Tong et al. [16], PCL as the carbon source of HAD required much shorter HRT and lower current intensity, which might be due to a shortage of methanol, or because the liquid-phase carbon source dosage was difficult to control. However, PCL could provide a sufficient carbon source for denitrification via continuous hydrolysis by microorganisms. Furthermore, PCL also acted as a biological carrier to increase the biomass in the reactor, which was conducive to the denitrification.

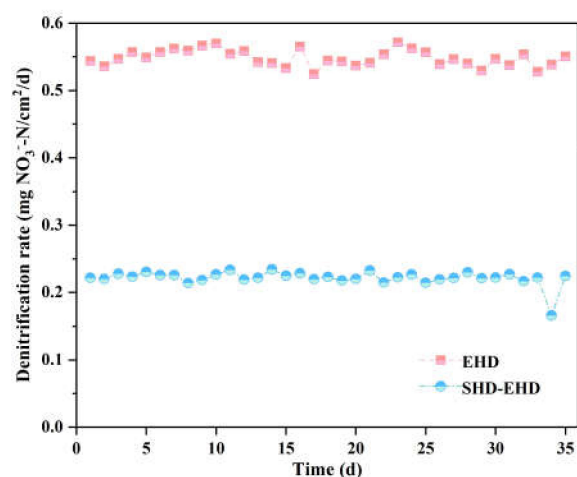


Figure 7. Comparison of denitrification rates of SHD–EHD and EHD under optimal conditions ($I = 40$ mA, HRT = 4 h, pH = 7.4~7.5, $\text{inf-NO}_3^- \text{-N} = 40$ mg/L).

Table 2. Comparison with other denitrification systems.

Reactors	$\text{inf-NO}_3^- \text{-N}$ (mg/L)	Current (mA)	HRT (h)	Removal Rate (%)	External Carbon Source	Cathode and Anode Material	Reference
HEAD-PBR	25	100	18	99.70	pine sawdust	cathode: stainless steel mesh anode: Ti/RuO ₂	[33]
HAD-BER	50	60	8	99.90	methanol	biological carrier: haycite cathode: stainless steel mes hanode: stainless steel bar	[16]
SHD-EHD	40	40	4	99.04	PCL	biological carrier: cotton fibers cathode: carbon felt anode: graphite rods biological carrier: PCL	This study
3DBER-SAD	35	60	12	92.00	-	cathode/anode: carbon rods biological carrier: activated carbon electron donor: sulfur	[35]

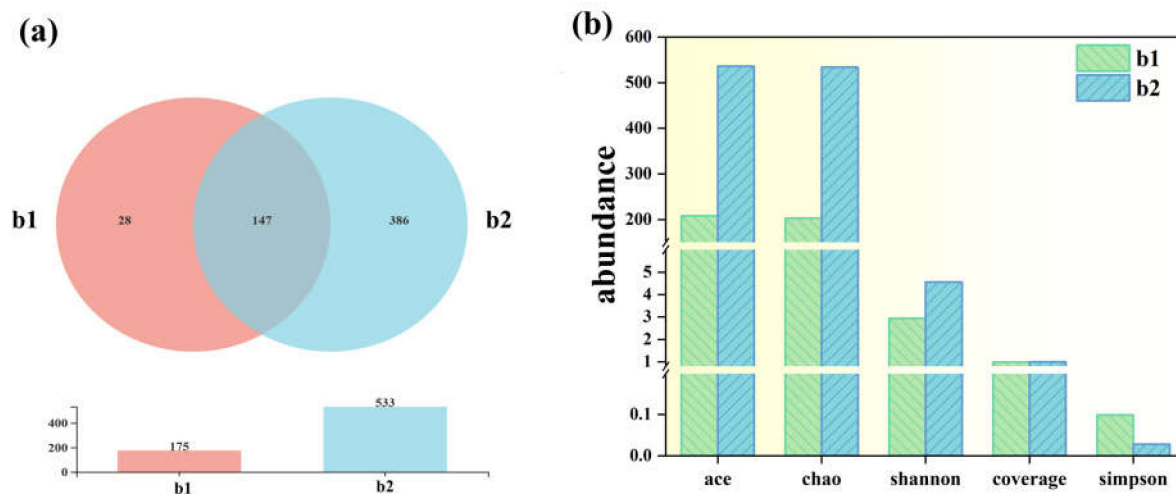
Compared with the SHD-EHD constructed in this study (Table 3), the conventional hydrogen autotrophic denitrification reactors required more energy consumption; the energy consumption of the SHD-EHD was reduced by 71.15–95.41% compared to them [36–38], which was 44.09% lower than the EHD in this study. These results indicated that the SHD-EHD could significantly reduce the energy consumption. In addition, although the energy consumption of the SHD-EHD was slightly higher than that of the HAD-BER with liquid carbon source [16], the SHD-EHD with PCL as a solid carbon source could be operated continuously without supplementing the carbon source, reducing the maintenance and operation costs.

Table 3. Comparison of energy consumption with previous denitrification systems.

Reactor Type	Denitrification Type	Energy Consumption (kWh/kg NO ₃ ⁻ -N)	Reference
multi-electrode BER	Hydrogen autotrophic	70	[36]
3D-BER	Hydrogen autotrophic	440	[37]
two-chambe BES	Hydrogen autotrophic	200	[38]
EHD	Hydrogen autotrophic	36.11	This study
HAD-BER	Heterotrophic/ hydrogen autotrophic	20	[16]
SHD-EHD	Heterotrophic/ hydrogen autotrophic	20.19	This study

3.7. Analysis of Microbial Community Structure

The 16S rRNA high-throughput sequencing was performed on the samples collected from the SHD-EHD (b1) and the solid-phase heterotrophic denitrification reactor (SHD) (b2), respectively, to investigate the abundance and diversity of the microbial communities. The bacterial community structures were also identified at the phylum and genus levels. The Venn diagram (Figure 8a) shows that the operational taxonomic units of the two samples b1 and b2 were 175 and 533, respectively, indicating that a large number of species in the SHD-EHD system were eliminated. The abundance indices (Ace and Chao) of the SHD were much higher than that of the SHD-EHD (Figure 8b), which suggests the similar conclusion that the microbial diversity homogeneity of the SHD reactor was significantly higher than that of the SHD-EHD. Nevertheless, the denitrification performance of the SHD-EHD was better than the SHD, which might be due to the electrical stimulation that promoted the proliferation of dominant denitrifying bacteria and electroactive bacteria.

**Figure 8.** (a) Venn diagram; (b) Diversity indexes of samples from SHD-EHD and SHD.

At the phylum level, microbial community composition and abundance were exhibited in Figure 9a. *Proteobacteria* was the dominant phylum (86.81%) in the SHD-EHD reactor. As previously reported, many types of denitrifying bacteria, such as *Thauera*, *Hydrogenophaga*, *Alcaligenes* and *Dechloromonas*, were affiliated with *Proteobacteria* [33]. In addition, as *Proteobacteria* in the SHD-EHD consisted of as high as 86.81% of the abundance; other phyla had a low abundance. In contrast, the phyla distribution in the SHD was more uniform, in which the abundance of the dominant phyla *Proteobacteria*, *Bacteroidota* and *Chloroflexi* reached 44.48%, 22.22% and 17.83%, respectively. It could be concluded that denitrifying bacteria could effectively adapt to an electrical environment and kept proliferating while bacteria without such ability were finally eliminated by electrical selection and lost in the competition with denitrifying bacteria. Therefore, high nitrate removal rate in the SHD-

EHD was achieved by high abundance of electrically enriched denitrifying bacteria. The results demonstrated that the bacterial community composition in the SHD-EHD could bring better nitrate removal rate, which reflects the significance of enriching denitrifying bacteria through electrical stimulation.

At the class level, most of the sequences in the SHD-EHD and the SHD belonged to 16 classes, among which *Gammaproteobacteria*, *Bacteroidia*, *Alphaproteobacteria*, *Anaerolineae* and *Chloroflexia* were the main ones (Figure 9b). *Gammaproteobacteria* had the largest proportion of all classes in both samples. The relative abundance of *Gammaproteobacteria* in SHD-EHD and SHD were 72.93% and 39.04%, respectively. *Gammaproteobacteria* included many denitrifying bacteria [39]; therefore, the abundance of *Gammaproteobacteria* was positively correlated with the denitrification performance. This suggested that the addition of PCL not only provided carbon source for denitrification, but also promoted the enrichment of denitrifying bacteria.

At the genus level, the main denitrifying bacteria in the SHD-EHD mainly included *Dechloromonas*, *Thauera*, *Hydrogenophaga* and *Acidovorax* (Figure 9c). *Dechloromonas* was the dominant genus with the highest abundance in the SHD-EHD, which could use organic carbon sources as electron donors to reduce O_2 , nitrate and nitrite under anoxic condition [40,41]. The relative abundance of *Dechloromonas* in the SHD-EHD increased compared to the SHD, probably due to the electrical stimulation that promoted its activity and improved its ability to utilize organic carbon sources. *Thauera* could not only utilize organic matters as carbon sources for heterotrophic denitrification, but also could use H_2 as an electron donor for hydrogen autotrophic denitrification [42]. The relative abundance of *Thauera* in the SHD-EHD and the SHD were 14.56% and 3.82%, respectively, indicating that electrical stimulation facilitated the enrichment of *Thauera*. Therefore, the SHD-EHD constructed in this study achieved autotrophic–heterotrophic synergistic denitrification. *Hydrogenophaga* in the SHD-EHD was from the *Comamonadacea* family, which was able to use H_2 for autotrophic growth [43]. H_2 generated at the cathode could be utilized by *Hydrogenophaga*. The inorganic carbon generated during the heterotrophic denitrification provided carbon sources for the growth of *Hydrogenophaga*. In consequence, the heterotrophic denitrifying bacteria could facilitate the growth of *Hydrogenophaga* in the SHD-EHD. *Acidovorax* with a relative abundance of 4.29% in the SHD-EHD had the ability to oxidize H_2 for denitrification [44]. In addition, small amounts of *Rhodopseudomonas* (3.21%) and *Alishewanella* (1.77%) were also found in the biofilm sample from the SHD-EHD. *Rhodopseudomonas* was able to fix nitrogen, produce H_2 and fix CO_2 [45]; it could remove NO_3^- -N probably by biological nitrogen fixation in denitrification system [46]. It was reported that *Alishewanella* had the ability to reduce NO_3^- -N [47]. In this study, the relative abundance of *Stenotrophomonas* was 0.04% in the SHD and 2.47% in the SHD-EHD, which demonstrated that H_2 generated by electrolysis promoted the enrichment of *Stenotrophomonas*. Moreover, it was reported that *Stenotrophomonas* could shuttle electrons generated during the oxidation of substrates via electron mediators or direct contact with the electrode. *Denitratisoma* was also found in the two reactors. A previous study showed that the accumulation of NO_2^- -N was low in an HAD system, owing to the high abundance of *Denitratisoma* in which the nitrite reductase could facilitated the reduction of NO_2^- -N [43].

In addition, there were some genera that had the abilities of degrading biodegradable polymer and denitrification. The denitrifying genus *Acidovorax* in the SHD-EHD was capable of both autotrophic denitrification and metabolism of PCL because of its potential to hydrolyze ester bonds [48,49]. This enabled *Acidovorax* to be enriched by an order of magnitude in the SHD-EHD, where PCL served as the solid carbon source. Moreover, the enrichment of *Bacteroidetes* might facilitate the hydrolysis of PCL, thus releasing small molecule carbon sources more favorable to denitrifying bacteria [50].

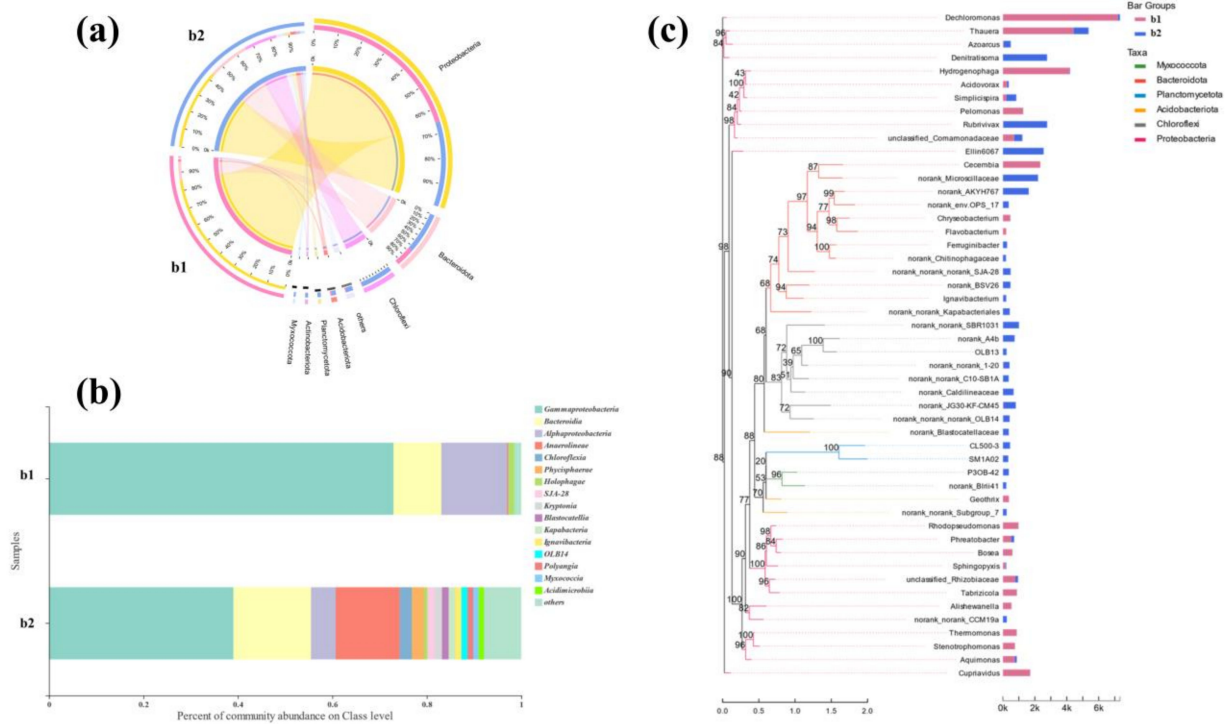


Figure 9. Relative abundance of samples at (a) Phylum level; (b) Class level; (c) Genus level.

3.8. Analysis of Metabolic Pathway

The nitrogen metabolic pathway was predicted by combining the gene data from the metagenome sequencing results with the nitrogen metabolism information from the KEGG database (Figure 10). Four related denitrifying enzymes appeared in both samples, which were iso-nitrate reductase (narG, narH and napA), nitrite reductase (nirK and nirS), nitric oxide reductase (norB and norC) and nitrous oxide reductase (nosZ). The abundance of enzymes in the SHD-EHD was higher than in the SHD, representing more active denitrification in the SHD-EHD. According to previous results, the SHD-EHD displayed a better nitrate removal rate. Therefore, electrical stimulation increased the activity of nitrate reductase and nitrite reductase, which was consistent with former study [13]. Nitrate reductases were represented by membrane-bound nitrate reductase (narG and narH) and periplasmic nitrate reductase (napA). Although napA was a peritroplasmic nitrate reductase, its distance from the outer membrane was shorter than that of narG and narH, and it could be connected to external electron flow [51]. Therefore, the expression of napA was expected to increase at a high current intensity. However, the expression of napA decreased while narG and narH expression increased at high current intensity. This might be due to the gene regulation, which had not evolved for adapting to the change of carbon source [52], or narG and narH increased the electron utilization for the reduction of NO_3^- -N, rather than for respiration.

NosZ was proposed to be the rate-limiting step in the whole denitrification pathway. The low expression of nosZ might lead to the accumulation of N_2O . The accumulation of denitrifying intermediates except N_2O was not observed. The gene expression data of nitrite reductase was in correspondence with the effluent NO_2^- -N concentration. The accumulation of NO_2^- -N was not observed after NO_3^- -N was reduced to NO_2^- -N at all current intensities, representing that the expression of nirK and nirS gradually increased to saturation with the increase of current intensity. The nitrite reductase byproduct NO might not accumulate because it was unstable and was easily converted to N_2O or other forms through abiotic processes. In addition, the expression data of norB and norC suggested that bioconversion of NO to N_2O might have been greatly activated. Finally, from the accumulation of N_2O

and the low expression of *nosZ*, it was concluded that the transformation of NO to N₂O was the rate-limiting step in the whole denitrification pathway.

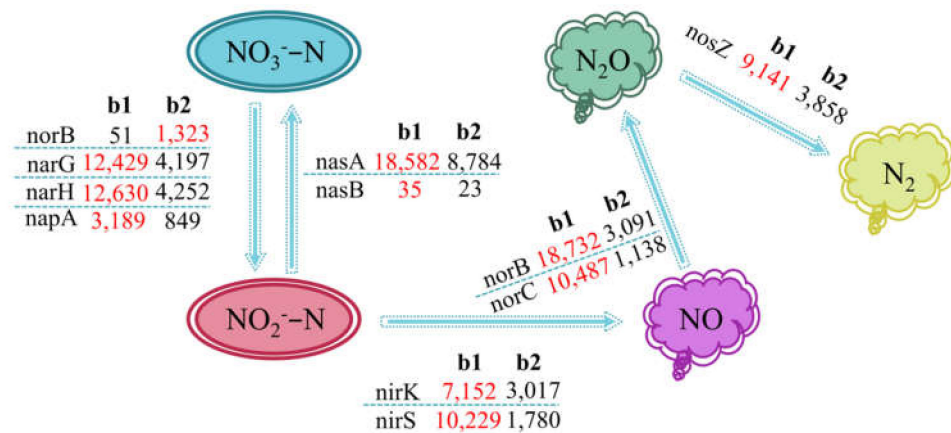


Figure 10. Nitrogen metabolism pathway analysis.

3.9. Material Conversion and Mechanism

As a biodegradable polymer, PCL could be decomposed by microbial enzymes. In the SHD-EHD, the PCL acted as an electron donor for heterotrophic denitrification Equation (3) and the carrier for the attachment of microorganisms as well. The decomposition product CO₂ could be used as the carbon source for autotrophic denitrification.

In the lower part of the SHD-EHD, dissolved oxygen was consumed by electrochemical reaction Equation (4), creating an anoxic environment for denitrifying bacteria. At the same time, H₂ generated through electrolysis served as the electron donor for autotrophic denitrification Equations (5) and (6). The anodic carbon rod was oxidized to generate CO₂ Equation (7), offering the carbon source required for autotrophic denitrification for denitrifying bacteria. Autotrophic denitrification was the main process of inorganic carbon consumption.

As described above, the SHD-EHD was a collaborative system combining multiple processes. The possible pathway of material transformation in the SHD-EHD was listed as follows (the transformation approach in the SHD-EHD was shown in Figure 11):

1. *In situ* H₂ production at the cathode was consumed for autotrophic denitrification.
2. NO₃⁻ and NO₂⁻ produced by electrochemical denitrification and incomplete denitrification were transformed into N₂ mainly by heterotrophic and autotrophic denitrification.
3. Part of NO₃⁻-N was assimilated by microorganisms and transformed to organic nitrogen.
4. PCL could be hydrolyzed by microorganisms into an organic carbon source that could be easily utilized by heterotrophic microorganisms.
5. Organic carbon was transformed into inorganic carbon by microbial hydrolysis, metabolism and heterotrophic denitrification, which provided a carbon source for autotrophic denitrification, thus achieving synergistic heterotrophic and autotrophic denitrification in the SHD-EHD.

Efficient material transformation was achieved by the combination of solid-phase heterotrophic denitrification and electrochemical hydrogen autotrophic denitrification. Satisfactory nitrate removal performance and low concentrations of by-products were realized, providing a novel and efficient method for nitrate removal.

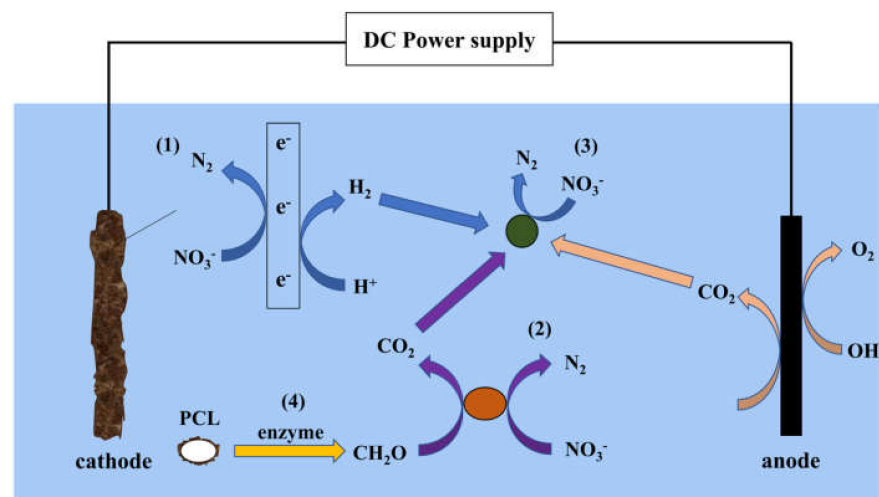


Figure 11. Denitrification mechanism in the SHD–EHD: (1) Electrochemical denitrification reduction; (2) Heterotrophic denitrification; (3) Hydrogen autotrophic denitrification; (4) Hydrolysis of PCL.

4. Conclusions

In summary, a heterotrophic denitrification coupled with electro-autotrophic denitrification system was developed for treating nitrate-contaminated groundwater, in which PCL served as the carbon source. Under the optimal condition (influent nitrate concentration of 40 mg/L, current intensity of 40 mA and HRT of 4 h), a high nitrate removal rate of 99.04% could be realized. Compared with the EHD, the SHD-EHD with PCL facilitated the complete denitrification and reduced the accumulation of NO_2^- -N. *Dechloromonas*, *Thauera* and *Hydrogenophaga* were identified as the key denitrifying bacteria in the SHD-EHD. Comparison of microbial communities from the SHD-EHD and the SHD revealed that electrical stimulation boosted the abundance of the dominant denitrifying bacteria and the electroactive bacteria. The conversion of NO to N_2O was the rate-limiting step in the overall denitrification pathway, according to the analysis of the nitrogen metabolic pathway. The SHD-EHD developed in this study shows promising potential for the removal of nitrate from groundwater. However, further study on the generation of intermediate gases and synergistic removal with other pollutants in the SHD-EHD is required to explain the detailed nitrate removal mechanisms of the SHD-EHD.

Supplementary Materials: The following supporting information can be downloaded at: <https://www.mdpi.com/article/10.3390/w14111759/s1>, Figure S1: Denitrification performance of EHD under optimal conditions; DNA extraction and Illumina MiSeq sequencing; Figure S2: SEM of carbon felt in SHD-EHD: (a) bare carbon felt; (b) carbon felt after reaction; Figure S3: Effect of different current on NO_3^- -N and NO_2^- -N concentrations; Figure S4: Effect of different HRT on NO_3^- -N and NO_2^- -N concentrations; Figure S5: Effect of different pH on NO_3^- -N and NO_2^- -N; Figure S6: Effect of influent pH on anode, cathode and effluent pH of EHD; Figure S7: Effect of different inf- NO_3^- -N on NO_3^- -N and NO_2^- -N concentrations.

Author Contributions: Conceptualization, X.T.; methodology, S.Y.; investigation, S.Y.; resources, X.T. and S.Z.; writing—original draft preparation, S.Y. and L.L.; writing—review and editing, X.T. and L.L.; supervision, X.T.; funding acquisition, X.T. All authors have read and agreed to the published version of the manuscript.

Funding: This research was funded by the National Natural Science Foundation of China (No. 21806126) and the Fundamental Research Funds for the Central Universities (WUT.2019IVB031).

Informed Consent Statement: Not applicable.

Data Availability Statement: Not applicable.

Acknowledgments: The advice of microbial analysis from Hao-Jin Peng in School of Civil Engineering and Architecture, Wuhan University of Technology, China is gratefully acknowledged.

Conflicts of Interest: The authors declare no conflict of interest.

References

1. United Nations. The United Nations World Water Development Report 2022: Groundwater: Making the Invisible Visible. Available online: https://digitallibrary.un.org/record/3967679?ln=zh_CN (accessed on 23 March 2022).
2. Arjen, H.; Ashok, C.; Pieter, V.O. Advancing Water Footprint Assessment Research: Challenges in Monitoring Progress towards Sustainable Development Goal 6. *Water* **2017**, *9*, 438.
3. Ghafari, S.; Hasan, M.; Aroua, M.K. Effect of carbon dioxide and bicarbonate as inorganic carbon sources on growth and adaptation of autohydrogenotrophic denitrifying bacteria. *J. Hazard. Mater.* **2009**, *162*, 1507–1513. [[CrossRef](#)] [[PubMed](#)]
4. Ballantine, K.A.; Groffman, P.M.; Lehmann, J.; Schneider, R.L. Stimulating nitrate removal processes of restored wetlands. *Environ. Sci. Technol.* **2014**, *48*, 7365–7373. [[CrossRef](#)] [[PubMed](#)]
5. Garcia-Segura, S.; Lanzarini-Lopes, M.; Hristovski, K.; Westerhoff, P. Electrocatalytic reduction of nitrate: Fundamentals to full-scale water treatment applications. *Appl. Catal. B: Environ.* **2018**, *236*, 546–568. [[CrossRef](#)]
6. Wang, H.; Chen, N.; Feng, C.; Deng, Y. Insights into heterotrophic denitrification diversity in wastewater treatment systems: Progress and future prospects based on different carbon sources. *Sci. Total Environ.* **2021**, *780*, 146521. [[CrossRef](#)]
7. Liang, J.; Chen, N.; Tong, S.; Liu, Y.; Feng, C. Sulfur autotrophic denitrification (SAD) driven by homogeneous composite particles containing CaCO₃-type kitchen waste for groundwater remediation. *Chemosphere* **2018**, *212*, 954–963. [[CrossRef](#)]
8. Feng, H.; Huang, B.; Zou, Y.; Li, N.; Wang, M.; Yin, J.; Cong, Y.; Shen, D. The effect of carbon sources on nitrogen removal performance in bioelectrochemical systems. *Bioresour. Technol.* **2013**, *128*, 565–570. [[CrossRef](#)]
9. Molognoni, D.; Deveseri, M.; Cecconet, D.; Capodaglio, A.G. Cathodic groundwater denitrification with a bioelectrochemical system. *J. Water Process Eng.* **2017**, *19*, 67–73. [[CrossRef](#)]
10. Tang, Y.; Ziv-El, M.; Meyer, K.; Zhou, C.; Shin, J.H.; Ahn, C.H.; McQuarrie, J.; Candelaria, D.; Swaim, P.; Scott, R.; et al. Comparing heterotrophic and hydrogen-based autotrophic denitrification reactors for effluent water quality and post-treatment. *Water Supply* **2012**, *12*, 227–233. [[CrossRef](#)]
11. Kiss, I.; Szekeres, S.; Bejerano, T.T.; Soares, M.I.M. Hydrogen-dependent denitrification: Preliminary assessment of two bioelectrochemical systems. *Water Sci. Technol.* **2000**, *42*, 373–379. [[CrossRef](#)]
12. Zhao, Y.X.; Feng, C.P.; Wang, Q.H.; Yang, Y.N.; Zhang, Z.Y.; Sugiura, N. Nitrate removal from groundwater by cooperating heterotrophic with autotrophic denitrification in a biofilm-electrode reactor. *J. Hazard. Mater.* **2011**, *192*, 1033–1039. [[CrossRef](#)] [[PubMed](#)]
13. Liu, H.Y.; Tong, S.; Chen, N.; Liu, Y.; Feng, C.P.; Hua, Q.L. Effect of electro-stimulation on activity of heterotrophic denitrifying bacteria and denitrification performance. *Bioresour. Technol.* **2015**, *196*, 123–128. [[CrossRef](#)] [[PubMed](#)]
14. Zhai, S.Y.; Ji, M.; Zhao, Y.X.; Pavlostathis, S.G.; Zhao, Q. Effects of salinity and COD/N on denitrification and bacterial community in dicyclic-type electrode based biofilm reactor. *Chemosphere* **2018**, *192*, 328–336. [[CrossRef](#)] [[PubMed](#)]
15. Ghafari, S.; Hasan, M.; Aroua, M.K. Nitrate remediation in a novel upflow bio-electrochemical reactor (UBER) using palm shell activated carbon as cathode material. *Electrochim. Acta* **2009**, *54*, 4164–4171. [[CrossRef](#)]
16. Tong, S.; Zhang, B.; Feng, C.; Zhao, Y.; Chen, N.; Hao, C.; Pu, J.; Zhao, L. Characteristics of heterotrophic/biofilm-electrode autotrophic denitrification for nitrate removal from groundwater. *Bioresour. Technol.* **2013**, *148*, 121–127. [[CrossRef](#)]
17. Liu, H.Y.; Hu, Q.L. Analysis of denitrification performance and microbial community structure in a bio-electrochemical reactor under different current densities with wheat-rice stone powder. *Water Reuse* **2022**, *12*, 66–77. [[CrossRef](#)]
18. Zhao, Y.X.; Zhang, B.G.; Feng, C.P.; Huang, F.Y.; Zhang, P.; Zhang, Z.Y.; Yang, Y.N.; Sugiura, N. Behavior of autotrophic denitrification and heterotrophic denitrification in an intensified biofilm-electrode reactor for nitrate-contaminated drinking water treatment. *Bioresour. Technol.* **2012**, *107*, 159–165. [[CrossRef](#)]
19. Zhang, J.M.; Feng, C.P.; Hong, S.Q.; Hao, H.L.; Yang, Y.N. Behavior of solid carbon sources for biological denitrification in groundwater remediation. *Water Sci. Technol.* **2012**, *65*, 1696–1704. [[CrossRef](#)]
20. Ribera-Guardia, A.; Kassotaki, E.; Gutierrez, O.; Pijuan, M. Effect of carbon source and competition for electrons on nitrous oxide reduction in a mixed denitrifying microbial community. *Process Biochem.* **2014**, *49*, 2228–2234. [[CrossRef](#)]
21. Wang, J.L.; Chu, L.B. Biological nitrate removal from water and wastewater by solid-phase denitrification process. *Biotechnol. Adv.* **2016**, *34*, 1103–1112. [[CrossRef](#)]
22. Zhong, Y.; Godwin, P.; Jin, Y.; Xiao, H. Biodegradable polymers and green-based antimicrobial packaging materials: A mini-review. *Adv. Ind. Eng. Polym. Res.* **2020**, *3*, 27–35. [[CrossRef](#)]
23. RameshKumar, S.; Shaiju, P.; O'Connor, K.E. Bio-based and biodegradable polymers—State-of-the-art, challenges and emerging trends. *Curr. Opin. Green Sustain. Chem.* **2020**, *21*, 75–81. [[CrossRef](#)]
24. Mergaert, J.; Boley, A.; Cnockaert, M.C.; Muller, W.R.; Swings, J. Identity and potential functions of heterotrophic bacterial isolates from a continuous-upflow fixed-bed reactor for denitrification of drinking water with bacterial polyester as source of carbon and electron donor. *Syst. Appl. Microbiol.* **2001**, *24*, 303–310. [[CrossRef](#)] [[PubMed](#)]
25. Chu, L.B.; Wang, J.L. Denitrification of groundwater using PHBV blends in packed bed reactors and the microbial diversity. *Chemosphere* **2016**, *155*, 463–470. [[CrossRef](#)] [[PubMed](#)]
26. Li, P.; Zuo, J.E.; Wang, Y.J.; Zhao, J.; Tang, L.; Li, Z.X. Tertiary nitrogen removal for municipal wastewater using a solid-phase denitrifying biofilter with polycaprolactone as the carbon source and filtration medium. *Water Res.* **2016**, *93*, 74–83. [[CrossRef](#)]

27. Zhang, Q.; Ji, F.; Xu, X. Effects of physicochemical properties of poly- ϵ -caprolactone on nitrate removal efficiency during solid-phase denitrification. *Chem. Eng. J.* **2016**, *283*, 604–613. [[CrossRef](#)]
28. Shen, Z.Q.; Yin, Y.N.; Wang, J.L. Biological denitrification using poly(butanediol succinate) as electron donor. *Applied Microbiol. Biotechnol.* **2016**, *100*, 6047–6053. [[CrossRef](#)]
29. Wu, W.Z.; Yang, L.H.; Wang, J.L. Denitrification using PBS as carbon source and biofilm support in a packed-bed bioreactor. *Environ. Sci. Pollut. Res.* **2013**, *20*, 333–339. [[CrossRef](#)]
30. Cui, Y.; Lai, B.; Tang, X.H. Microbial Fuel Cell-Based Biosensors. *Biosensors* **2019**, *9*, 18. [[CrossRef](#)]
31. Singh, B.K.; Quince, C.; Macdonald, C.A.; Khachane, A.; Thomas, N.; Abu Al-Soud, W.; Sorensen, S.J.; He, Z.L.; White, D.; Sinclair, A.; et al. Loss of microbial diversity in soils is coincident with reductions in some specialized functions. *Environ. Microbiol.* **2014**, *16*, 2408–2420. [[CrossRef](#)]
32. Jian-Cha, W. Enhanced Removal of Nitrogen and Phosphorus in 3DBER Filled with Sponge Iron and Activated Carbon. *China Water Wastewater* **2014**, *209*, 57–64. [[CrossRef](#)]
33. Peng, T.; Feng, C.P.; Hu, W.W.; Chen, N.; He, Q.C.; Dong, S.S.; Xu, Y.X.; Gao, Y.; Li, M. Treatment of nitrate-contaminated groundwater by heterotrophic denitrification coupled with electro-autotrophic denitrifying packed bed reactor. *Biochem. Eng. J.* **2018**, *134*, 12–21. [[CrossRef](#)]
34. Shen, Z.; Zhou, Y.; Wang, J. Comparison of denitrification performance and microbial diversity using starch/poly(lactic acid) blends and ethanol as electron donor for nitrate removal. *Bioresour. Technol.* **2013**, *131*, 33–39. [[CrossRef](#)] [[PubMed](#)]
35. Hao, R.X.; Meng, C.C.; Li, J.B. An integrated process of three-dimensional biofilm-electrode with sulfur autotrophic denitrification (3DBER-SAD) for wastewater reclamation. *Appl. Microbiol. Biotechnol.* **2016**, *100*, 7339–7348. [[CrossRef](#)] [[PubMed](#)]
36. Sakakibara, Y.; Nakayama, T. A novel multi-electrode system for electrolytic and biological water treatments: Electric charge transfer and application to denitrification. *Water Res.* **2001**, *35*, 768–778. [[CrossRef](#)]
37. Zhou, M.; Fu, W.; Gu, H.; Lei, L. Nitrate removal from groundwater by a novel three-dimensional electrode biofilm reactor. *Electrochim. Acta* **2007**, *52*, 6052–6059. [[CrossRef](#)]
38. Pous, N.; Koch, C.; Vila-Rovira, A.; Balaguer, M.D.; Colprim, J.; Muehlenberg, J.; Mueller, S.; Harnisch, F.; Puig, S. Monitoring and engineering reactor microbiomes of denitrifying bioelectrochemical systems. *Rsc Adv.* **2015**, *5*, 68326–68333. [[CrossRef](#)]
39. Feng, T.; Wu, J.; Chai, K.; Liu, F. Effect of *Pseudomonas* sp. on the degradation of aluminum/epoxy coating in seawater. *J. Mol. Liq.* **2018**, *263*, 248–254. [[CrossRef](#)]
40. Horn, M.A.; Ihssen, J.; Matthies, C.; Schramm, A.; Acker, G.; Drake, H.L. *Dechloromonas denitrificans* sp nov., *Flavobacterium denitrificans* sp nov., *Paenibacillus anaericanus* sp. nov and *Paenibacillus terrae* strain MH72, N₂O-producing bacteria isolated from the gut of the earthworm *Aporrectodea caliginosa*. *Int. J. Syst. Evol. Microbiol.* **2005**, *55*, 1255–1265. [[CrossRef](#)]
41. Coates, J.D.; Chakraborty, R.; Lack, J.G.; O'Connor, S.M.; Cole, K.A.; Bender, K.S.; Achenbach, L.A. Anaerobic benzene oxidation coupled to nitrate reduction in pure culture by two strains of *Dechloromonas*. *Nature* **2001**, *411*, 1039–1043. [[CrossRef](#)]
42. Zhang, Y.W.; Wei, D.Y.; Morrison, L.; Ge, Z.B.; Zhan, X.M.; Li, R.H. Nutrient removal through pyrrhotite autotrophic denitrification: Implications for eutrophication control. *Sci. Total Environ.* **2019**, *662*, 287–296. [[CrossRef](#)] [[PubMed](#)]
43. Xu, Z.S.; Dai, X.H.; Chai, X.L. Biological denitrification using PHBV polymer as solid carbon source and biofilm carrier. *Biochem. Eng. J.* **2019**, *146*, 186–193. [[CrossRef](#)]
44. Vasiliadou, I.A.; Pavlou, S.; Vayenas, D.V. Dynamics of a chemostat with three competitive hydrogen oxidizing denitrifying microbial populations and their efficiency for denitrification. *Ecol. Model.* **2009**, *220*, 1169–1180. [[CrossRef](#)]
45. Karpinets, T.V.; Pelletier, D.A.; Pan, C.L.; Uberbacher, E.C.; Melnichenko, G.V.; Hettich, R.L.; Samatova, N.F. Phenotype Fingerprinting Suggests the Involvement of Single-Genotype Consortia in Degradation of Aromatic Compounds by *Rhodospseudomonas palustris*. *PLoS ONE* **2009**, *4*, e4615. [[CrossRef](#)] [[PubMed](#)]
46. Du, L.; Trinh, X.; Chen, Q.R.; Wang, C.; Wang, H.H.; Xia, X.; Zhou, Q.H.; Xu, D.; Wu, Z.B. Enhancement of microbial nitrogen removal pathway by vegetation in Integrated Vertical-Flow Constructed Wetlands (IVCWs) for treating reclaimed water. *Bioresour. Technol.* **2018**, *249*, 644–651. [[CrossRef](#)]
47. Morris, J.M.; Jin, S.; Crimi, B.; Pruden, A. Microbial fuel cell in enhancing anaerobic biodegradation of diesel. *Chemical Eng. J.* **2009**, *146*, 161–167. [[CrossRef](#)]
48. Nalcaci, O.O.; Boke, N.; Ovez, B. Potential of the bacterial strain *Acidovorax avenae* subsp *avenae* LMG 17238 and macro algae *Gracilaria verrucosa* for denitrification. *Desalination* **2011**, *274*, 44–53. [[CrossRef](#)]
49. McIlroy, S.J.; Kirkegaard, R.H.; McIlroy, B.; Nierychlo, M.; Kristensen, J.M.; Karst, S.M.; Albertsen, M.; Nielsen, P.H. MiDAS 2.0: An ecosystem-specific taxonomy and online database for the organisms of wastewater treatment systems expanded for anaerobic digester groups. *Database J. Biol. Databases Curation* **2017**. [[CrossRef](#)]
50. Zhang, D.Y.; Vahala, R.K.; Wang, Y.; Smets, B.F. Microbes in biological processes for municipal landfill leachate treatment: Community, function and interaction. *Int. Biodeterior. Biodegrad.* **2016**, *113*, 88–96. [[CrossRef](#)]
51. Simpson, P.J.L.; Richardson, D.J.; Codd, R. The periplasmic nitrate reductase in *Shewanella*: The resolution, distribution and functional implications of two NAP Isoforms, NapEDABC and NapDAGHB. *Microbiology. SGM* **2010**, *156*, 302–312. [[CrossRef](#)]
52. Doan, T.V.; Lee, T.K.; Shukla, S.K.; Tiedje, J.M.; Park, J. Increased nitrous oxide accumulation by bioelectrochemical denitrification under autotrophic conditions: Kinetics and expression of denitrification pathway genes. *Water Res.* **2013**, *47*, 7087–7097. [[CrossRef](#)] [[PubMed](#)]